GRANT
NAG-1-943
38001
P.36

Noise Characteristics of Passive Components for Phased Array Applications

M. Kemal Sönmez and Robert J. Trew

High Frequency Electronics Laboratory
Department of Electrical and Computer Engineering
North Carolina State University
Raleigh, N.C. 27695-7911

for

NASA Langley Research Center

Report on Grant NAG-1-943

(NASA-CR-187219) NOISE CHARACTERISTICS OF PASSIVE COMPONENTS FOR PHASED ARRAY APPLICATIONS Progress Report, period ending [illegible] 1991 (North Carolina State Univ.) [illegible] CSCL 20A G3/71

N91-30707

Unclas
0039001

TABLE OF CONTENTS

I. INTRODUCTION

Twenty years ago, it was asserted that "more than 40 percent of the noise in low-noise communication systems and 95 percent of the noise in low-noise radio astronomy receivers is due to "black body" radiation from passive linear elements"[1]. Today, with the advent of the new very low-noise active components (e.g. HEMT's), the effect of the passive components on the noise performance is even more emphasized. In a phased array application, combiners and transmission lines which transfer the power from the antennae to the circuitry, and the phase shifters which steer the beam are among the most important components in the noise performance of the whole system. In this report, results of a comparative study on noise characteristics of basic power combining/dividing and phase shifting schemes are presented.

The second section deals with the theoretical basics of thermal noise in a passive linear multiport. Theory of thermal noise from a linear passive multiport is well established.[1,4]. Many of the relations needed to analyze the noise behavior of the passive circuits are available and there is little room for theoretical improvement. Still, we present a new formalism to describe the noise behavior of passive circuits and show that the fundamental results (the most fundamental being Bosma's theorem) are conveniently achieved using this description. The formalism has not yielded any new results yet, but it has provided a fresh insight into the noise wave scattering analysis. It has also pointed to a new direction of research, namely, the application of the Transmission Line Matrix (TLM) method to the analyses of noise scattering in an environment containing both passive and active distributed noise sources. The possibilities of application are discussed in the Future Research Goals

section.

The third section contains the results of analyses concerning the noise behavior of basic power combining/dividing structures. The studied structures are the Wilkinson combiner, 90° hybrid coupler, hybrid ring coupler and the Lange coupler. The effect of material selection is also addressed by comparing the noise performances of five different types of substrates in order to form a representative group for a wide range of substrates used in practice.

In the fourth section, three types of PIN-diode switch phase shifters are analyzed in terms of noise performance. A complete comparison would, of course, have to include active phase shifters. This prospect is discussed in the Future Research Goals section.

This report mainly summarizes the first efforts in comparing the noise performances of different structures using a circuit approach. Such an approach is, by its circuit nature, restricted to the circuit analysis tools and element models available in CAD programs. These tools may not always be the best way to address the noise problem. The next objective is, by using the proposed formulation for noise waves, to get a field-theoretical grip on the subject and produce our own software tools to model the sources of noise like radiation which are difficult to handle with circuit analysis software. The proposed TLM method, being a genuine time-domain method, is adequate to model even transient noise phenomena and to account for radiation which is enhanced by the multiple reflections inside the circuit.

II. Theory of Noise Waves in Passive Linear Multiports

The representation of noise in terms of waves has proven to be a quite useful tool in the noise analyses of microwave circuits [6]-[8]. The standard wave representation of a noisy multiport is

$$\mathbf{b} = \mathbf{S}\mathbf{a} + \mathbf{c} \tag{1}$$

where $\mathbf{a}$ is the incident wave, $\mathbf{b}$ is the reflected wave and $\mathbf{c}$ is the outgoing noise wave contributed by the network. $\mathbf{S}$ is the scattering matrix.

Noise characterization of a multiport can be made in terms of its correlation matrix $\mathbf{C_s}$ defined as

$$\mathbf{C_s} = \overline{\mathbf{c}\mathbf{c}^\dagger} \tag{2}$$

where the dagger and the overbar stand for a Hermitian transpose and time average, respectively. Scattering matrix and the noise wave correlation matrix are sufficient to give a complete description of the electrical behavior of a multiport [1]. The noise figure at port j of a multiport with reflectionless ports is given by

$$NF_j = 1 + \frac{C_{sjj}}{kT_0 \sum_{i \neq j} |S_{ji}|^2} \tag{3}$$

where T_0 is the reference temperature.

The purpose of this section is to provide a mathematical tool to investigate the scattering of noise waves *inside* a multiport. The noisy components inside a physical multiport are distributed and require infinitely many differential lumped elements for a distributed

parameter representation. The equivalent noise sources associated with these differential elements, therefore, also constitute a set of finite measure. Scattering matrix theory, which is limited to countable number of ports is not suitable for treating the scattering of noise waves produced by the set of differential noise sources distributed throughout the multiport. Bounded linear operators on a Hilbert space are proposed as *scattering operators* to deal with the distributed nature of the noise sources. This is discussed in Sec. II.A The Hilbert space and bounded linear operators on this space are described in Sec. II.B Such an approach may be useful to make finer noise performance evaluations of microwave components in applications where noise is of utmost importance such as low loss radiometers. In such an application, this approach makes it possible to include radiation as a source of noise. It may also be used in physical modelling of noise generation in various components.

The formulation is used in Sec. II.C to derive the noise correlation matrix of a passive multiport in terms of its temperature and scattering matrix. This has been discussed by Bosma and termed the "noise distribution matrix"[1], and recently has been derived in an elegant way by Wedge *et al.*[4] The merit of the present derivation is its conceptual simplicity i.e., regarding **c** as the combined effect of all the dissipative processes in the system. This is, of course, made possible by the representation of these processes in a comprehensive Hilbert space structure. The lack of correlation between reflected waves on which the derivation in [4] is based follows as a corollary to Bosma's theorem which, in this work, is proved directly by extracting the physical sources of noise, namely dissipative elements.

II.A. Thermal Noise in Passive Distributed Multiports

A multiport is defined to be passive if the only power that can be extracted from it is the thermally radiated noise power [1]. The thermal noise in a multiport is wholly due to the dissipative processes in the multiport as asserted by the generalized Nyquist relation [5]. Therefore, resistance, which is the representation of dissipation in electrical circuits is sufficient to model the noise sources inside the multiport.

The idea of representing noise sources in a passive linear multiport by M resistances, then regarding these sources as terminations to an $N + M$ port is quite well-known. It has been used to derive the Nyquist thorem [2], and to demonstrate the bounded-real properties of the scattering matrix [3]. In both cases, however, it has been limited to the case where the multiport consists of an interconnection of a finite number of lossless subnetworks and resistances. This is the limit imposed by the scattering matrix theory which is by its very nature restricted to a countable number of ports. A physical passive multiport is, however, distributed due to the random processes responsible for noise generation. Lumped elements like resistors, capacitors, inductors, transformers or gyrators are mathematical idealizations, and a complete description of the properties of any element can only be given when it is represented as an interconnection of infinitely many differential elements. The simplest example of this is the RLCG parameters of a transmission line which constitute an infinite set of differential elements.

In the next section, we present an operator formalism for multiports with any number of ports using a Hilbert space structure. Bounded linear operators on the Hilbert space are the natural generalizations of matrices in the N-dimensional space. This formalism

allows us to represent the infinitely many noise sources as ports to a "big" multiport and treat the "big" multiport using *scattering operators*. We specify a particular Hilbert space for linear distributed multiports as the region of applicability for the scattering operators. This approach has been developed to address the scattering of noise waves in a distributed environment and is useful to gain insight about the distribution of noise power inside the multiport.

II.B. Hilbert Space

The motivation of the following setting is to replace the matrices in N dimensional space with their natural generalizations, bounded linear operators in Hilbert space. We define the Hilbert space $H = \mathbf{C}^N \times L^2(\Theta)$, the elements of which can be represented by column vectors of the form

$$\mathbf{A} = \begin{pmatrix} \mathbf{a} \\ f_a \end{pmatrix}$$

where $\mathbf{a} \in \mathbf{C}^N$ and $f_a \in L^2(\Theta)$. Θ is a finite measure subset of $\mathbf{R}$. We have an inner product and a norm on this space defined as

$$< \mathbf{A}, \mathbf{B} >= \sum_{i=1}^{N} a_i b_i^* + \int_\Theta d\tau f_a(\tau) f_b^*(\tau) \ ,$$

$$||\mathbf{A}|| = \sqrt{< \mathbf{A}, \mathbf{A} >} \ .$$

where the integral is in the Lebesgue sense. In this way, the measure on the direct product space is a combination of Lebesgue and counting measures. The proofs of claims about the space, the inner product and the norm are straightforward.

A linear operator $\mathbf{\Lambda}$ on H can be defined as a matrix of linear transformations

$$\mathbf{\Lambda} = \begin{pmatrix} \mathbf{\Lambda}_{11} & \mathbf{\Lambda}_{12} \\ \mathbf{\Lambda}_{21} & \mathbf{\Lambda}_{22} \end{pmatrix}$$

$\mathbf{\Lambda}_{11}$ and $\mathbf{\Lambda}_{22}$ are linear operators on $\mathbf{C}^N$ and $L^2(\Theta)$, respectively. $\mathbf{\Lambda}_{12}$:$L^2(\Theta) \longmapsto \mathbf{C}^N$, and $\mathbf{\Lambda}_{21}$:$\mathbf{C}^N \longmapsto L^2(\Theta)$ are linear tranformations. We denote the $N \times N$ identity matrix by $\mathbf{I_N}$ and the identity operator on $L^2(\Theta)$ by $\mathbf{I_{L^2}}$. So the identity operator on H is given by

$$\mathbf{I_H} = \begin{pmatrix} \mathbf{I}_N & \mathbf{0}_N \\ \mathbf{0}_N^T & \mathbf{I}_{L^2} \end{pmatrix}$$

where $\mathbf{0}_N$ is a N-column vector of zeros.

An element $\mathbf{A}$ of the Hilbert space corresponds to the noise wave amplitude defined by Bosma [1] for the "big" multiport. Accordingly, the power density at a frequency f is given by $< \mathbf{A}, \mathbf{A} >= ||\mathbf{A}||^2$.

II.C. Derivation of Bosma's Theorem

In this derivation, we assume everything in the passive multiport is distributed which is the physical case. We assume the multiport is at the uniform temperature T and is in thermodynamic equilibrium with its environment. Let Θ be the set of all the resistances in the multiport. We form a new multiport by regarding each of these resistances as terminations to $o(\Theta)$ ports of the new multiport. Each new port is normalized to the resistance value in which it is terminated. The new multiport has $N + o(\Theta)$ ports and is lossless since all the dissipative elements have been removed. $\mathbf{S}$, $\mathbf{a}$, $\mathbf{b}$ refer to the scattering matrix, the incident wave and the reflected wave of the N-port. $f_a(x)$ and $f_b(x)$ represent the incident and the reflected waves of the port x of the $N + o(\Theta)$-port (Fig. 1). For the new multiport,

a *scattering operator* $\mathbf{\Omega} : H \longmapsto H$ is defined as in Sec. III,

$$\begin{pmatrix} \mathbf{b} \\ f_b(x) \end{pmatrix} = \begin{pmatrix} \mathbf{S} & \int_\Theta d\tau \mathbf{p}(\tau)(\cdot) \\ \mathbf{q}^T(x) & \int_\Theta d\tau \omega(x,\tau)(\cdot) \end{pmatrix} \begin{pmatrix} \mathbf{a} \\ f_a(\tau) \end{pmatrix}. \tag{4}$$

This is simply the generalization of the scattering matrix of a finite multiport to an operator for a multiport with infinite number of "inner" ports in addition to N physical ports. $\mathbf{\Omega}_{11} = \mathbf{S}$ because of the normalization involved. The column vector of functions $\mathbf{q}(\mathbf{x})$ is defined as

$$q_i(x) = \frac{f_b(x)}{a_i}|_{a_j=0, j\neq i, f_a=0}. \tag{5}$$

The column vector of functions $\mathbf{p}(\mathbf{x})$, and $\omega(x,\tau)$ are defined as the kernels to the following Hilbert-Schmidt integral operators when $\mathbf{a} = \mathbf{0}_N$:

$$\mathbf{b} = \int_\Theta d\tau \mathbf{p}(\tau) f_a(\tau) \ , \tag{6}$$

$$f_b(x) = \int_\Theta d\tau \omega(x,\tau) f_a(\tau). \tag{7}$$

Since the $N+o(\Theta)$-port is lossless, input noise power must equal the output noise power. In the Hilbert space this is expressed as $< \mathbf{A}, \mathbf{A} >=< \mathbf{\Omega A}, \mathbf{\Omega A} >$ i.e., $||\mathbf{\Omega A}|| = ||\mathbf{A}||$. This shows that $\mathbf{\Omega}$ is non-singular. Combined with the fact that it is a linear operator, $\mathbf{\Omega}$ is thus shown to be a isomorphism of the Hilbert space onto itself i.e., a unitary operator. The adjoint of $\mathbf{\Omega}$, denoted as $\mathbf{\Omega}^\ddagger$, is thus guaranteed to exist and can easily be computed to give

$$\mathbf{\Omega}^\ddagger = \begin{pmatrix} \mathbf{S}^\dagger & \int_\Theta d\tau \mathbf{q}^*(\tau)(\cdot) \\ \mathbf{p}^\dagger(x) & \int_\Theta d\tau \omega^*(x,\tau)(\cdot) \end{pmatrix}. \tag{8}$$

Since $\mathbf{\Omega}$ is unitary, we have

$$\mathbf{\Omega}\mathbf{\Omega}^\ddagger = \mathbf{\Omega}^\ddagger\mathbf{\Omega} = \mathbf{I_H}. \tag{9}$$

Writing (9) using the matrix definitions (4) and (8), we get:

$$\begin{pmatrix} \mathbf{S}\mathbf{S}^\dagger + \int d\tau \mathbf{p}(\tau)\mathbf{p}^\dagger(\tau) & \mathbf{S}\int d\tau \mathbf{q}^*(\tau)(\cdot) + \int\int d\mu d\tau \mathbf{p}(\mu)\omega^*(\mu,\tau)(\cdot) \\ \mathbf{q}^T(x)\mathbf{S}^\dagger + \int d\tau \omega(x,\tau)\mathbf{p}^\dagger(\tau) & \mathbf{q}^T(x)\int d\tau \mathbf{q}^*(\tau)(\cdot) + \int\int d\mu d\tau \omega(x,\mu)\omega^*(\mu,\tau)(\cdot) \end{pmatrix} = \begin{pmatrix} \mathbf{I_N} & \mathbf{0}_N \\ \mathbf{0}_N^T & \mathbf{I_{L2}} \end{pmatrix}. \tag{10}$$

From (1) and (3), $\mathbf{c}$ can be written as the superposition of contributions from all the noise sources,

$$\mathbf{c} = \int_\Theta d\tau \mathbf{p}(\tau) f_a(\tau). \tag{11}$$

Then the correlation matrix $\mathbf{C}_s$ is given by

$$\mathbf{C}_s = \int_\Theta \int_\Theta d\mu d\tau \mathbf{p}(\mu)\mathbf{p}^\dagger(\tau)\overline{f_a(\mu)f_a^*(\tau)}. \tag{12}$$

The discrete resistances inside the multiport produce uncorrelated noise waves and the power spectral density of each source is given by its equipartition value. This gives

$$\overline{f_a(\mu)f_a^*(\tau)} = kT\delta_{\mu\tau}. \tag{13}$$

Substituting (13) into (12), we get

$$\mathbf{C}_s = kT\int_\Theta d\tau \mathbf{p}(\tau)\mathbf{p}^\dagger(\tau). \tag{14}$$

Bosma's Theorem is obtained upon substituition from (9):

$$\mathbf{C}_s = kT(\mathbf{I}_N - \mathbf{S}\mathbf{S}^\dagger). \tag{15}$$

We can summarize the preceding discussion as follows: By introducing scattering operators on a Hilbert space, it is possible to describe the scattering of noise waves from infinitely many sources in a distributed domain. In a passive multiport, in which all the noise sources are resistors, this mathematical formalism provides a convenient way to show

that the noise wave correlation matrix is given by Bosma's theorem. The formalism is useful for application in the high frequency spectrum where all elements are, by nature, distributed.

II.D. Noise Figure Formula for a Passive Multiport

Noise figure at a port of an N-port network is defined as the ratio of the total noise at that port over the transmitted input noise. The total noise consists of the transmitted noise plus the noise contributed by the network. The transmitted noise is the portion of the incident noise which passes through the system. When the noise figure is calculated at a port, the other ports in the network are terminated in their respective impedances. The noise figure at port j of a multiport with reflectionless ports is thus given by

$$NF_j = 1 + \frac{|c_j|^2}{k \sum_{i \neq j} |S_{ji}|^2 T_i} \tag{16}$$

where T_i is the temperature of the i-th port. Furthermore in section II.C. we showed that for a passive multiport at a uniform temperature T

$$\overline{\mathbf{cc}^\dagger} = kT(\mathbf{I}_N - \mathbf{SS}^\dagger). \tag{17}$$

Using this result (Bosma's Theorem), the noise figure at port j can easily be shown to be

$$NF(j) = 1 + \frac{T(1 - \sum_{i=1}^{N} |S_{ji}|^2)}{\sum_{i=1, i \neq j}^{N} T_i |S_{ji}|^2} \tag{18}$$

If all the ports are at the same temperature.i.e. $T_i = T_a, i = 1, \ldots, N$,The noise figure simplifies to:

$$NF(j) = \frac{T_a - T}{T_a} + \frac{T}{T_a} \frac{1 - |S_{jj}|^2}{\sum_{i=1, i \neq j}^{N} |S_{ji}|^2} \tag{19}$$

Finally, if $T = T_a$(thermodynamic equilibrium), we get:

$$NF(j) = \frac{1 - |S_{jj}|^2}{\sum_{i=1, i \neq j}^{N} |S_{ji}|^2} \tag{20}$$

The comparisons between various structures in the next sections have been realized assuming thermodynamic equilibrium with the understanding that different port temperatures can be taken into account using (18) and do not introduce new physics.

III. Coupling Structures

Our general approach will be to analyze the noise performances of a variety of combining/dividing structures first in the reflectionless case at thermodynamic equilibrium with the understanding that the different temperatures at different ports affect the noise figure through (2) but do not introduce new physics. Then we look into the mismatch problem for the basic structures.

Performances of five substrates for microstrip implementation of various combiners/dividers in the 1-12 GHz frequency range are analyzed, establishing some guidelines for choice of material and type of combining/dividing structure for operation with minimum noise. The effect of the mismatch on the noise contribution of these passive networks is investigated within the framework of the absorptive loss formulation.

III.A. 2-way Power Combiners and Dividers

Microwave power combining techniques which have been analyzed for noise performance in this work follow the classification made by Russell in his review paper[10]. Common forms of power combiner couplers given in [10] are Wilkinson combiner(2-way),Branch line 90 hybrid,Rat race, and Coupled line directional coupler. In our study, we analyzed Lange couplers as representative of coupled line structures. As a representative of a typical medium, Alumina with $\epsilon_r = 10$ was selected and the circuits were designed to operate at 10 GHz center frequency. The following table summarizes the divider/combiner characteristics at the center frequeny as well as noise figure calculated. Plots of the quantities in the table are given in Figs. 2,3.

Dividers	BW(%)	NF(dB)	Ret. Loss(dB)	Ins. Loss(dB)	Isolation(dB)
Wilkinson	36	3	46	3	30
Branch-line	11	3	38	3	42
Hybrid-ring	23	3	40	2.8	54
Lange	large	3	22	2.8	20

Combiners	BW(%)	NF(dB)	Ret. Loss(dB)	Ins. Loss(dB)	Isolation(dB)
Wilkinson	large	0.025	30	3	30
Branch-line	11	0.05	38	3	42
Hybrid-ring	26	0.05	48	2.8	33
Lange	large	0.17	23	2.8	20

As can be observed from the table, the resistive termination of one of the ports results in a large noise figure in the divider structures.In the combiners, the resistive termination can not couple any power to the output port due to the isolation. The Wilkinson combiner produces the lowest noise performance of the combiners studied.This is because the decisive dissipative loss in a microstrip on Alumina is the conductor loss which increases as the length of line is incrased. The Wilkinson combiner having the shortest length of transmission line has the least noise figure.

The noise figures of the dividing structures may be unacceptable for most low-noise applications. Therefore, we looked at the performance of a modified set of dividers in which the principal noise source,i.e. the isolation resistor has been removed and the fourth port has simply been grounded. This results in a trade-off between noise performance and

isolation. For a divider, if the output ports are well-matched, lack of isolation may not be a problem. The performance of the modified structures are summarized in the following table and plotted in Fig. 4.

Mod. Dividers	BW(%)	NF(dB)	Ret. Loss(dB)	Ins. Loss(dB)	Isolation(dB)
Wilkinson	large	0.05	46	3	6
Branch-line	11	0.03	38	3	6
Hybrid-ring	23	0.15	38	2.8	6
Lange	large	0.32	20	2.8	8

The grounded structures exhibit a very low noise figure, but the isolation has deterioated as expected. Still, for some applications, it may be reasonable to expect that the reflection from the loads will be low and the isolation will suffice.

III.B. N-WAY COUPLING STRUCTURES

In [10], combining approaches are grouped in two main categories, (i) structures which combine N channels in a single step (N-way combiners), and (ii) structures composed of a tree(corporate) or chain (serial) connection of the basic two-way combiners discussed above.

Three types of 4-way structures have been studied: Wilkinson,radial and planar. The optimized line impedances for these structures was obtained from [11]. 4-way combiners are found to have the same noise figure.($NF \approx 0.05$). The Wilkinson structure is advantageous in that the return loss and isolation are better than those of the other two. However, it is inherently 3-dimensional and is not suitable for planar implementation. The Radial structure is the second best in terms of coupling characteristics, yet it is not truly 2-

dimensional either. The Planar structure has the least isolation (14 dB),but it can be implemented in 2-dimensions .

Combiners	BW(%)	NF(dB)	Ret. Loss(dB)	Ins. Loss(dB)	Isolation(dB)
4-way Wilkinson	large	0.052	32	6.1	35
Radial	large	0.052	21	6.1	22
Planar	large	0.052	19	6.1	14

Dividers	BW(%)	NF(dB)	Ret. Loss(dB)	Ins. Loss(dB)	Isolation(dB)
4-way Wilkinson	18	6.05	33	6.1	35
Radial	18	5.68	34	6.1	22
Planar	18	4.76	34	6.1	14

The trade-off between noise figure and isolation is also apparent in the 4-way dividers. This compromise, being a fundamental property of multiports with odd number of ports comes up in various examples.

Corporate structures of the basic configurations mentioned in the inroduction paragraph of this section have been analyzed for N=4 to compare the two approaches described above. Results are summarized in the following table.

Combiners	BW(%)	NF(dB)	Ret. Loss(dB)	Ins. Loss(dB)	Isolation(dB)
2-way Wilkinson	large	0.059	36	6.1	27
Hyb. ring	32	0.092	50	6.1	28
Lange	large	0.324	20	6.3	24

Dividers	BW(%)	NF(dB)	Ret. Loss(dB)	Ins. Loss(dB)	Isolation(dB)
2-way Wilkinson	40	6.03	47	6.1	27
Hyb. ring	26	6.09	43	6.1	28
Lange	large	6.11	22	6.3	24

The noise figures of the corporate structures are somewhat higher due to the longer lines involved. Still, these structures are planar and it may be advantageous to use for example corporate structure of 2-way Wilkinson combiner instead of the planar 4-way combiner where planar construction and high isolation are required.

III.C. Effects of Substrate Material

In the same way we compare the noise properties of the basic combiners with matched ports, we want to see how significant an effect material selection has on the noise properties of the network. In the presence of reflectionless ports absorptive and dissipative loss are indistinguishable [9], therefore dissipation properties of the circuit will be the decisive factor in determining the noise figure. The most straightforward way to observe these properties is to compare the attenuation coefficients of the transmission lines used. To this end, Wilkinson, Branch-line, and Hybrid-ring coupler circuits were designed on five different substrates ranging in dielectric constant from 2.5 to 10. The transmission medium used was microstrip. In microstrip, dissipation can be attributed to conductor losses, dielectric losses, radiation and surface-wave propagation [13]. Though radiation and surface-wave propagation do cause power loss due to the existence of discontinuties,bends and closely located lines, the main contribution to the attenuation factor is from the conductor and di-

electric losses. Furthermore, in the low-loss substrate configurations used widely in practice, dielectric loss is small compared to the conductor loss.

The circuits were designed to operate at 4 and 10 GHz, and the effects of substrate selection were studied at those frequencies. The general trend is shown with the Hybrid ring coupler example in Fig. 5. Quartz and RT/duroid 5500 have been the least noisy substrates in all cases. This reflects the desirability of low dielectric constant which allows the use of wide lines which in turn reduce the series loss. It is apparent that shunt losses have secondary effect as there is not a correlation between noise performance and the loss tangents. Alumina and RT/duroid 60105 with $\epsilon_r = 10$ have been the noisiest substrates. Alumina in most cases have turned out to be more noisy although its loss tangent is much less than that of RT/duroid 60105. This is attributed to the high surface roughness of Alumina which is an important factor in series resistance in a microstrip.

III.D. Sensitivity to Mismatch

So far, we have been dealing with circuits with matched ports in which the noise properties are entirely dependent upon the power loss occuring within the circuit. However, the absorption coefficient of the passive circuit which is the complete description of the noise contribution is a function of termination reflection coefficients as briefed in the introduction. In a practical system, a finite reflection coefficient not anticipated during the design process always exists. In most cases this may be the decisive factor in noise performance rather than the resistive losses addressed in the preceding sections. Therefore we would like to observe the noise figure at the output port of the combiners as a function of the reflection coefficients at the other ports. In the combiners (dividers), we take the first port to be

the output (input) port, and the other N ports as input (output) ports. We assume the N input (output) ports have the same reflection coefficient which is a valid assumption for most combining (dividing) applications, e.g. an array of identical antennae. The variation of the noise figure at an output port over the complex input reflection plane is computed and plotted in Fig. 6 for the four basic combining structures. It is observed that the 2-way Wilkinson has the least sensitivity to the changes in reflection coefficient. Hybrid ring structure also performs fairly well under mismatch conditions. However, the noise figures of the Branch line coupler and the Lange coupler increase rapidly as the magnitude of the reflection coefficient gets larger. This result is in accordance with the frequency responses of the basic structures except for that of the Lange coupler reflecting the fact that operating the circuit at an off-resonance point is equivalent to having a larger reflection coefficient. The Lange combiner is fundamentally a broad band structure, still in the presence of mismatch it produces the largest noise of the four.

IV. Phase Shifters

A phase shifter is a two-port network in which the phase difference between the signals at the two ports can be controlled by a control signal (dc bias). The classification of phase shifter designs is given in [14]. In our first attempt to compare the noise behavior of various phase shifters, we will restrict our attention to digital PIN-diode phase shifters. Three phase shifter designs, one of the reflection type and two of the transmission type have been designed on an Alumina substrate using microstrip lines to operate at a frequency of 4 GHz. The reflection type phase shifter uses a hybrid 90° coupler to operate as a two-port. The transmission type of phase shifters are the switched-line type and the loaded-line type. All three components have been designed to provide one bit 45° phase shift. The Fig. 7 shows the circuits used. The PIN-diode used is a MA47899-030 whose equivalent circuit is shown in Fig. 8. The performance characteristics of the three phase shifters are summarized in the following tables:

Phase Shifters	BW(%)	RL^0(dB)	RL^1(dB)	IL^0(dB)	IL^1(dB)
Switched-line	20.0	34	36	0.193	0.194
Loaded-line	11.0	50	43	0.020	0.082
Reflection-type	6.8	38	32	0.138	0.287

Phase Shifters	NF^0(dB) center	NF^1(dB) center	NF^0(dB) max	NF^1(dB) max
Switched-line	0.192	0.192	0.204	0.196
Loaded-line	0.020	0.082	0.024	0.112
Reflection-type	0.137	0.284	0.142	0.287

In the above tables, ^{0} and ^{1} correspond to the two states of the phase shifter bit. The percent bandwidth is defined as the range of frequencies with phase shift error less than 10 % and return loss less than 20 dB.

From the above table, it may be observed that the loaded-line bit has superior noise performance and reasonable bandwidth. The switched-line coupler has a considerably larger bandwidth, but the noise figure throughout the band is significantly larger. The reflection-type design gives the worst performance in this case. The center frequency of 4 GHz is not suitable to design a reflection-type phase shifter bit with this particular diode. Also of importance is the offset between the noise figure values at different positions of the phase shifter bit in loaded-line and switched-line bits. In a phased array radiometry application where the noise generated in the circuitry has to be taken into account to make precise measurements, this offset leads to many different noise figures as the beam is steered in a digital manner. Switched-line phase shifter bit, having the same noise figure for both positions may be desirable if the situation described above is to be avoided.

V. Future Research Goals

The first phase of this study has been in the form of extending theory to gain insight into the noise problem in general. A Hilbert space formalism for modelling the distributed noise sources has been developed and it has been shown to provide convenient ways to prove the fundamental results of the present theory. It may be observed that the distributed noise sources represented by the formalism can be active or passive,i.e. thermal or some other kind of noise like shot noise. The noise analyses of the basic passive components in a phased array system have been carried out in a circuit context. Such an approach is limited to the capabilities of the CAD software at hand and cannot be easily extended to arbitrary shapes or configurations. The next goal is to have a field-theoretical grip on the noise wave scattering in a passive structure. The proposed method is the application of the time-domain TLM method to the noise wave scattering. The TLM method will also be able to address problems like transient inconsostencies of the components and the radiation brought about by the reflections caused by these. Up till now, the elements of the system have been evaluated seperately, and clearly, such an approach does not address the inter-system mismatches problem. Therefore, it is intended to take up complete systems and evaluate the system noise performance as a whole. This should provide further clues as to what kind of components function properly together, and what configuration is best for a certain selection of components.

V. REFERENCES

[1] H. Bosma,"On the Theory of Linear Noisy Systems," *Philips Res. Repts. Suppl.*, no. 10,1967.

[2] W.B.Davenport, W.L.Root *An Introduction to the Theory of Random Signals and Noise.* New York: IEEE Press, 1987.

[3] R.W.Newcomb *Linear Multiport Synthesis.* New York: McGraw-Hill, 1966.

[4] S.W.Wedge, D.B.Rutledge, "Noise Waves and Passive Linear Multiports" *IEEE Microwave and Guided Wave Letters.*, vol. 1, pp. 117-119, May 1991.

[5] H.B.Callen, T.A.Welton, "Irreversibility and Generalized Noise" *Physical Review.*, vol. 83, pp.34-40, July 1951.

[6] P.Penfield "Wave representation of amplifier noise," *IRE trans. Circuit Theory*, vol. CT-9, p.84, Mar. 1962.

[7] R.P.Meys, "A wave approach to the noise properties of linear microwave devices," *IEEE Trans. Microwave Theory Tech.*, vol. MTT-26, pp. 34-37, Jan. 1978.

[8] R.P. Hecken, "Analysis of linear noisy two-ports using scattering waves," *IEEE Trans. Microwave Theory Tech.*, vol. MTT-29, pp. 997-1004, Oct. 1981.

[9] D. Wait,"Thermal noise from a passive linear multiport," *IEEE Trans. Microwave Theory Tech.*, vol. MTT-16, no. 9, pp. 687-691, Sept. 1968.

[10] K. J. Russell,"Microwave power combining techniques," *IEEE Trans. Microwave The-*

ory *Tech.*, vol. MTT-27, no. 5, pp. 472-478, May 1979.

[11] A. A. M. Saleh, "Planar electrically symmetric n-way hybrid power dividers/combiners," *IEEE Trans. Microwave Theory Tech.*, vol. MTT-28, no. 6, pp. 555-563, June 1980.

[12] H. Bosma,"On the Theory of Linear Noisy Systems," *Philips Res. Repts. Suppl.*, no. 10,1967.

[13] T. C. Edwards, *Foundations for Microstrip Circuit Design.* New York: John Wiley & Sons, 1981.

[14] I. Bahl, P. Bhartia, *Microwave Solid State Circuit Design.* New York: John Wiley & Sons, 1988.

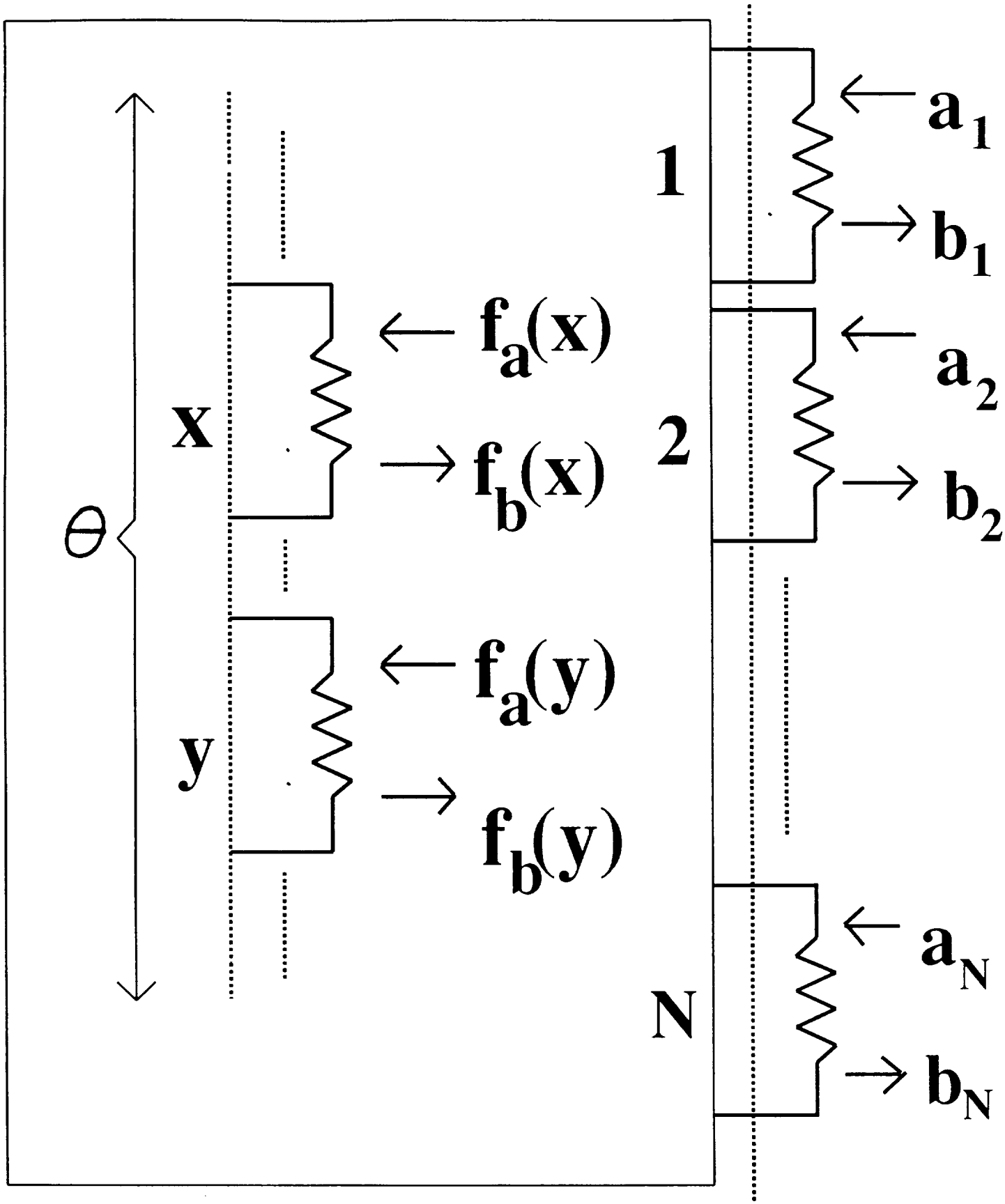

Fig. 1 Extraction of Distributed Resistances

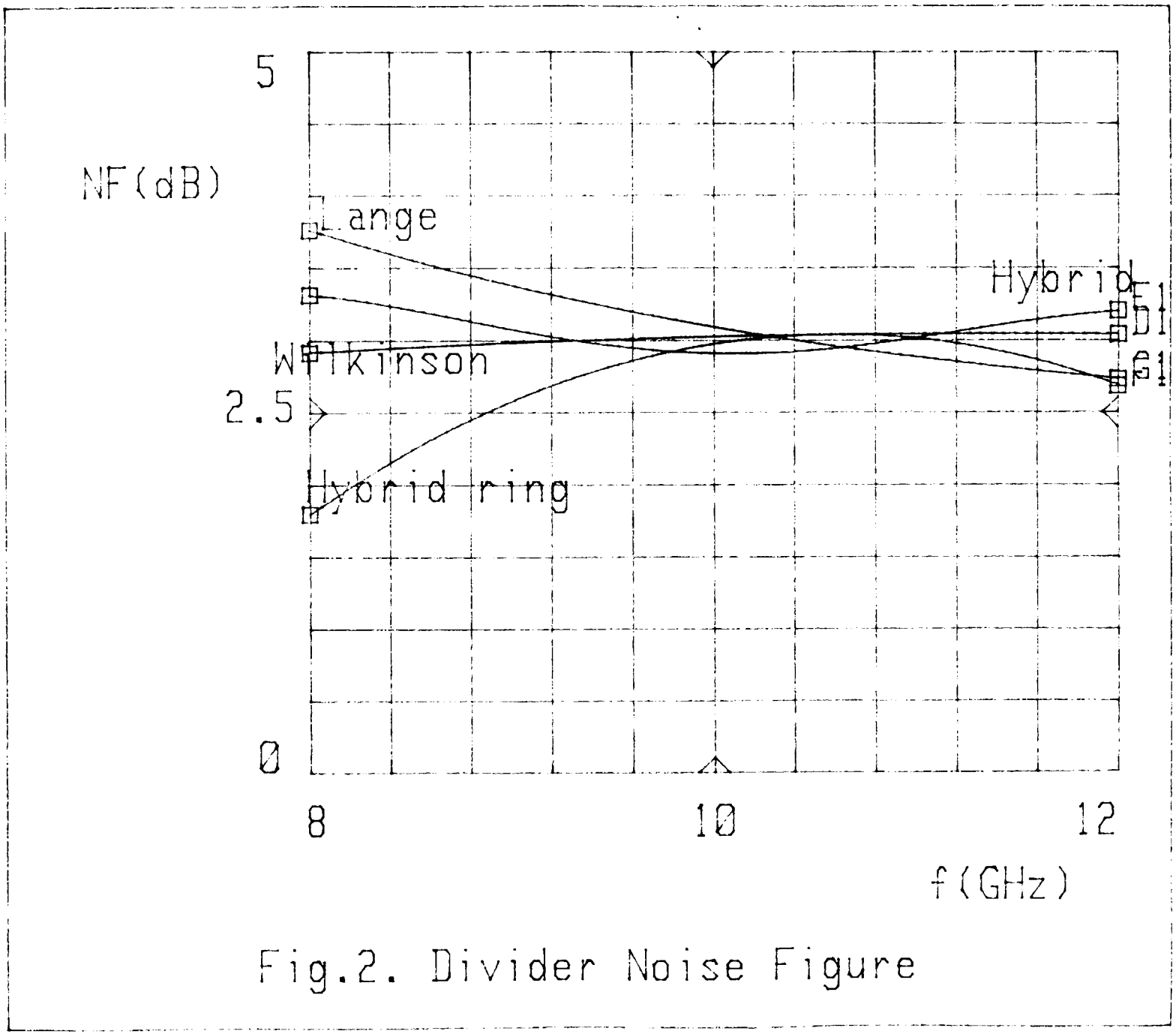

Fig.2. Divider Noise Figure

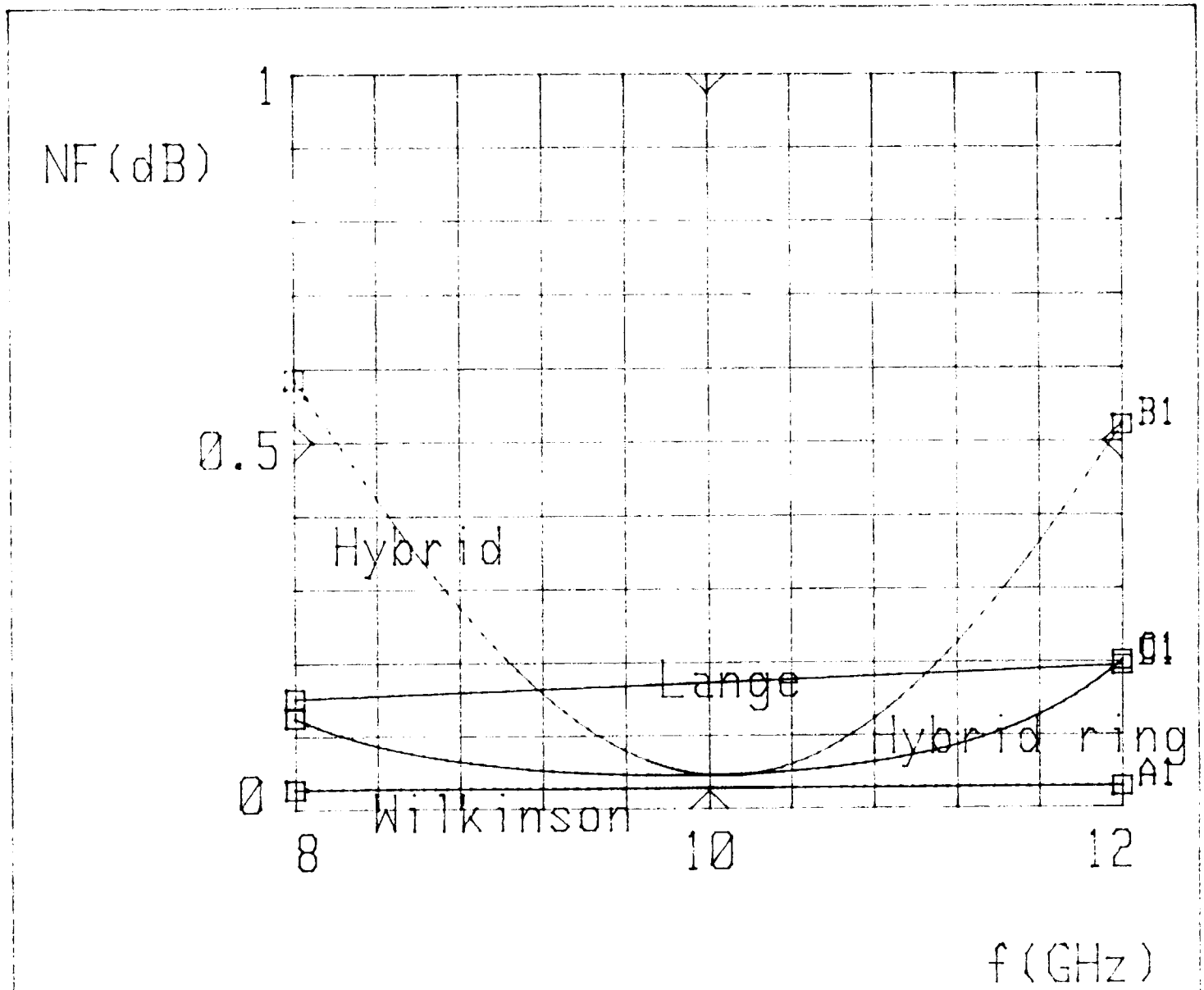

Fig. 3. Combiner Noise Figure

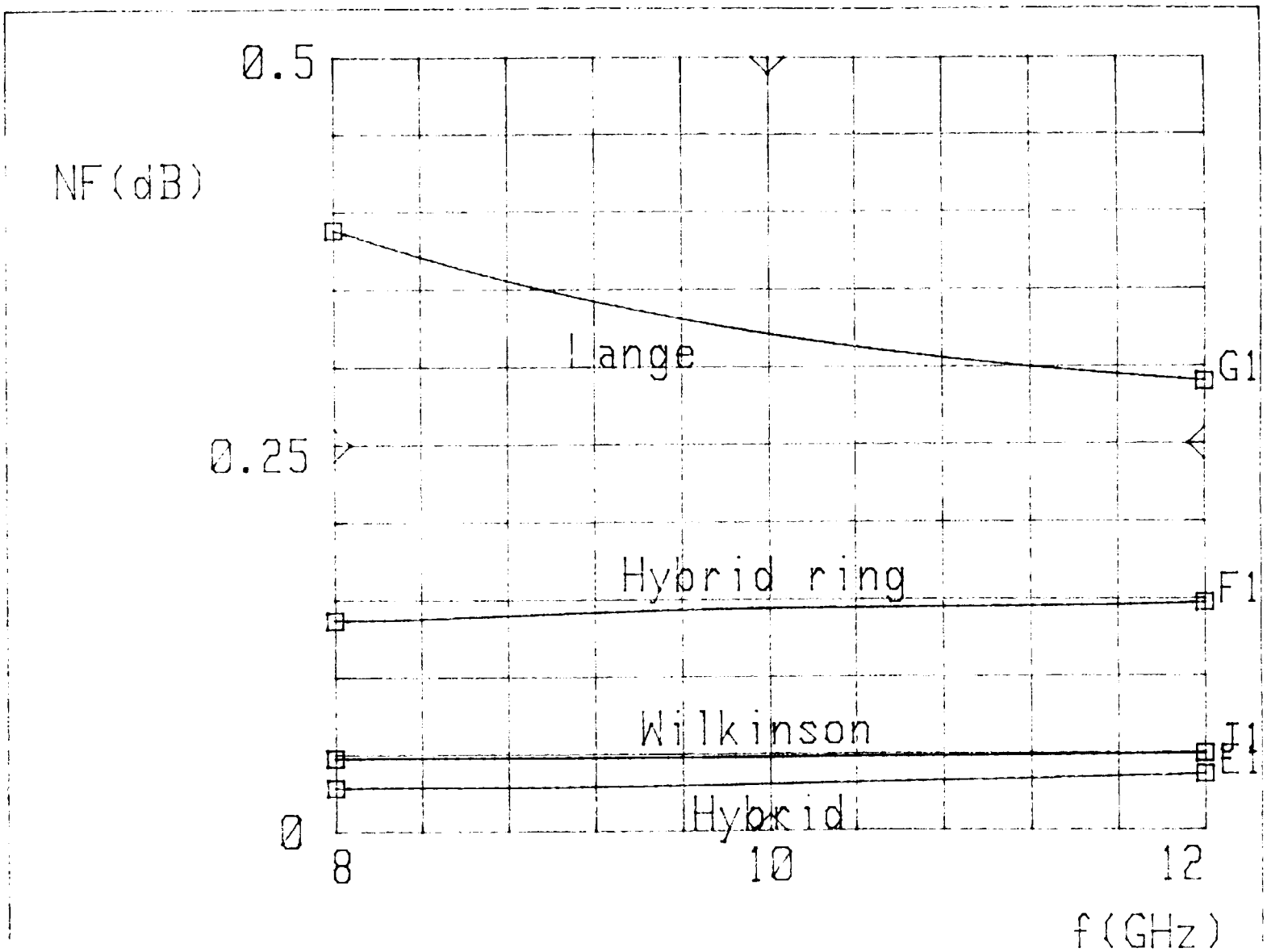

Fig. 4. Modified Divider Noise Figure

Substrates: RT/duroid 5500(a),6006(b),6010.5(c),quartz(d),alumina(99.5%)(e)

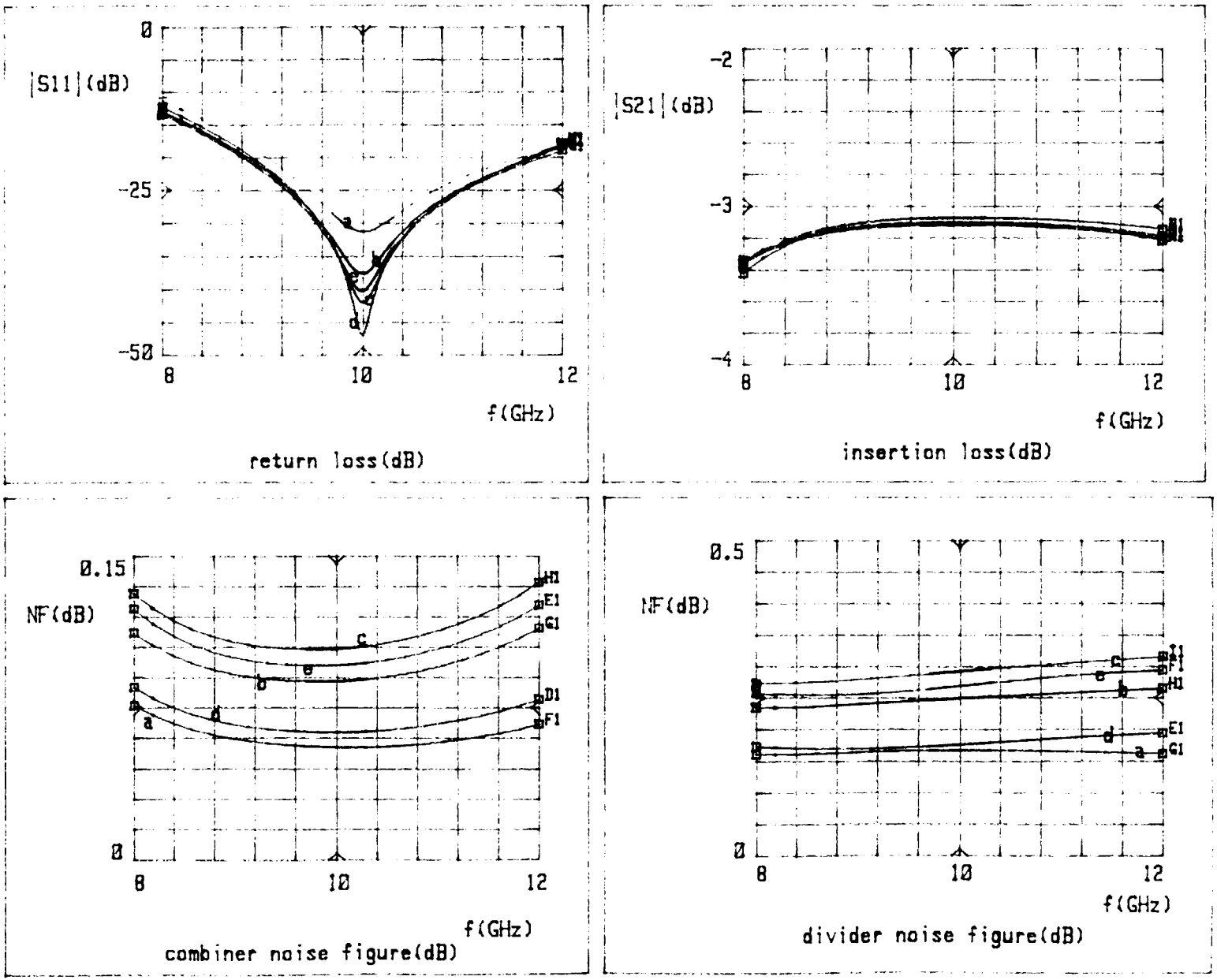

Fig.5. Performance of Hybrid ring couplers on various substrates

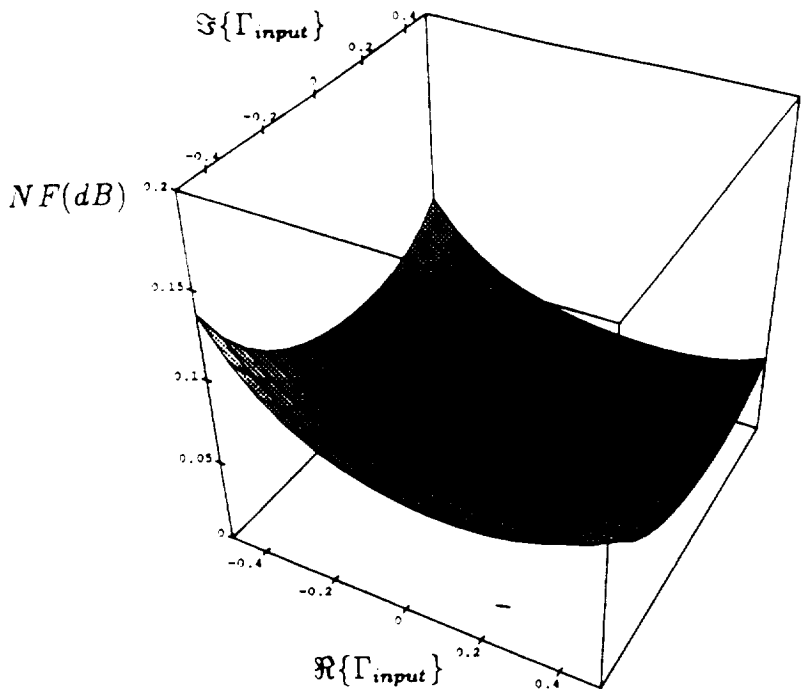

(a) 2-way Wilkinson combiner

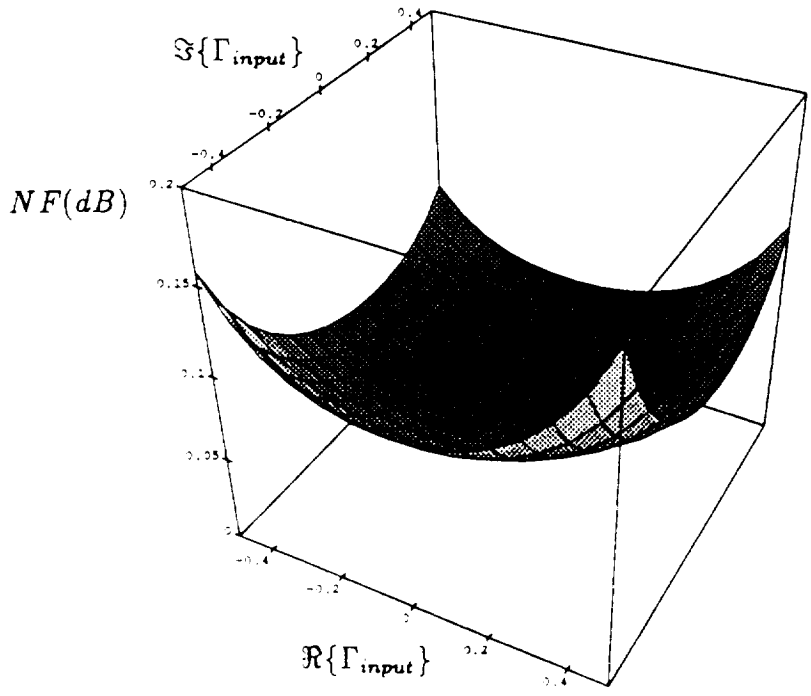

(b) Hybrid ring coupler

Fig. 6. Noise Figure at the output as a function of Γ_{input}

ORIGINAL PAGE IS
OF POOR QUALITY

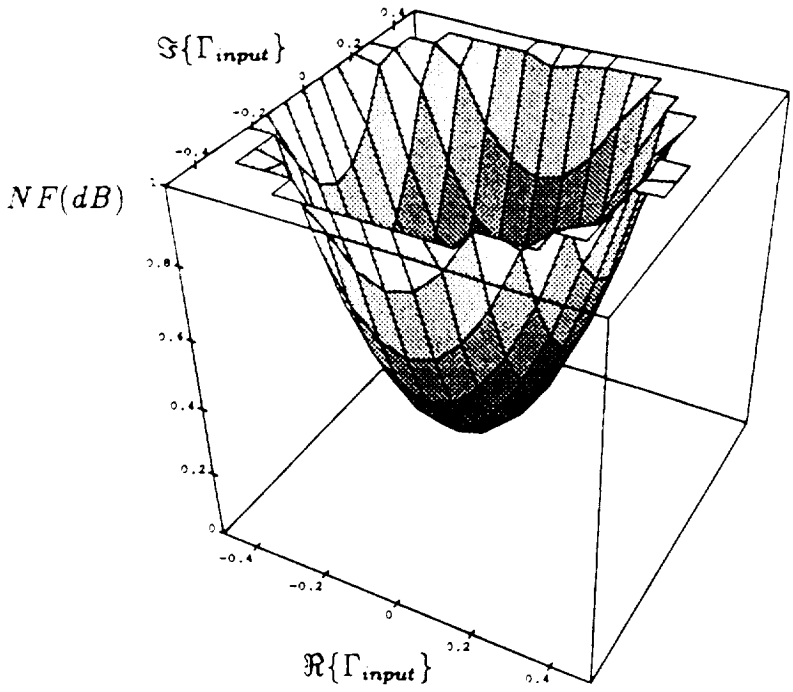

(c) Lange coupler

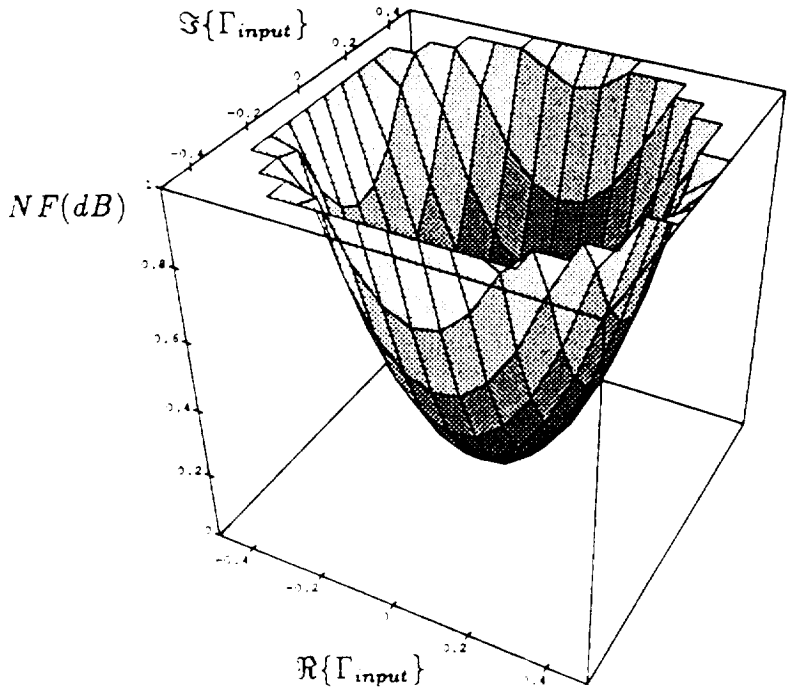

(d) Branch-line coupler

ORIGINAL PAGE IS
OF POOR QUALITY

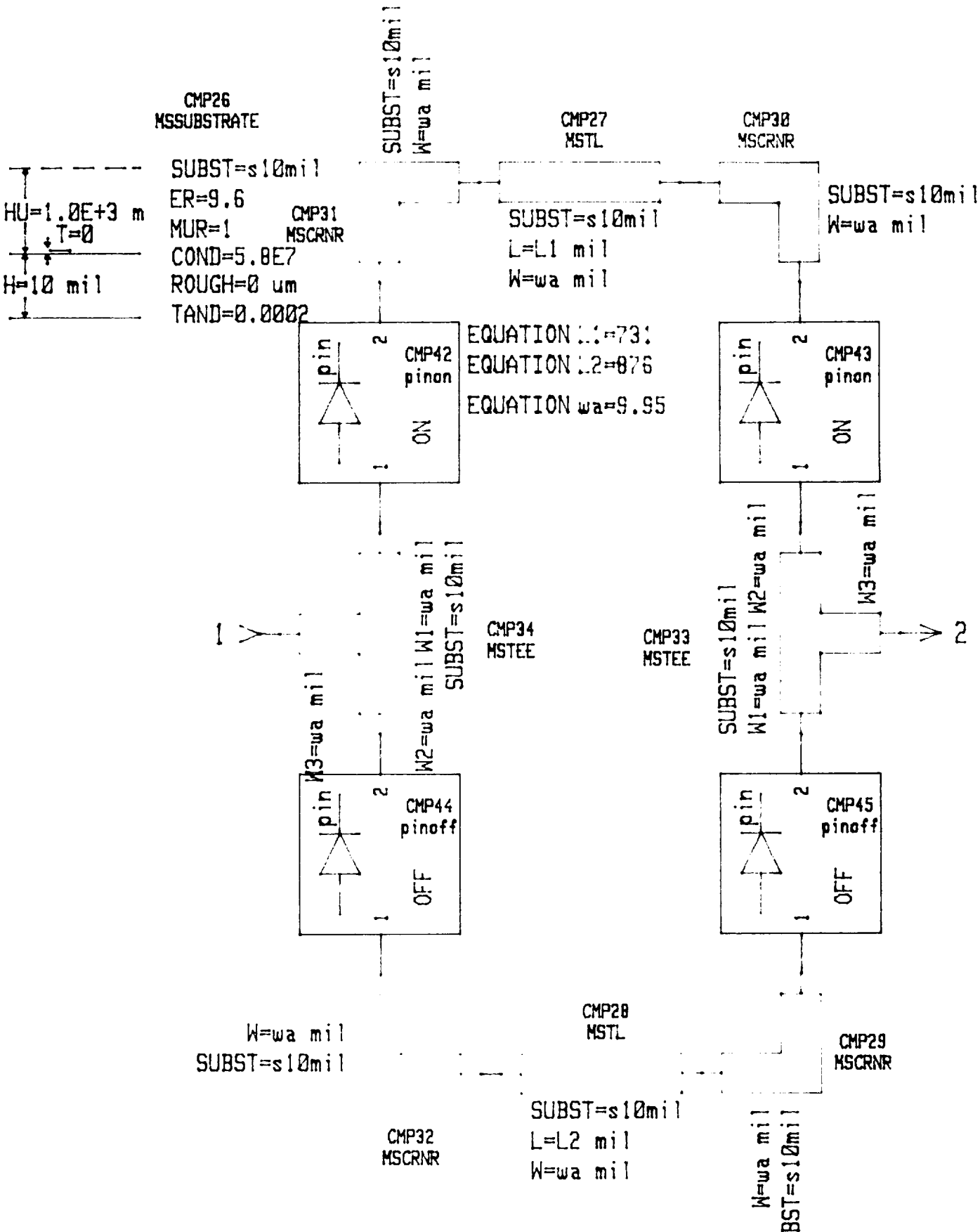

Fig. 7.a. Switched-Line Phase Shifter

ORIGINAL PAGE IS
OF POOR QUALITY

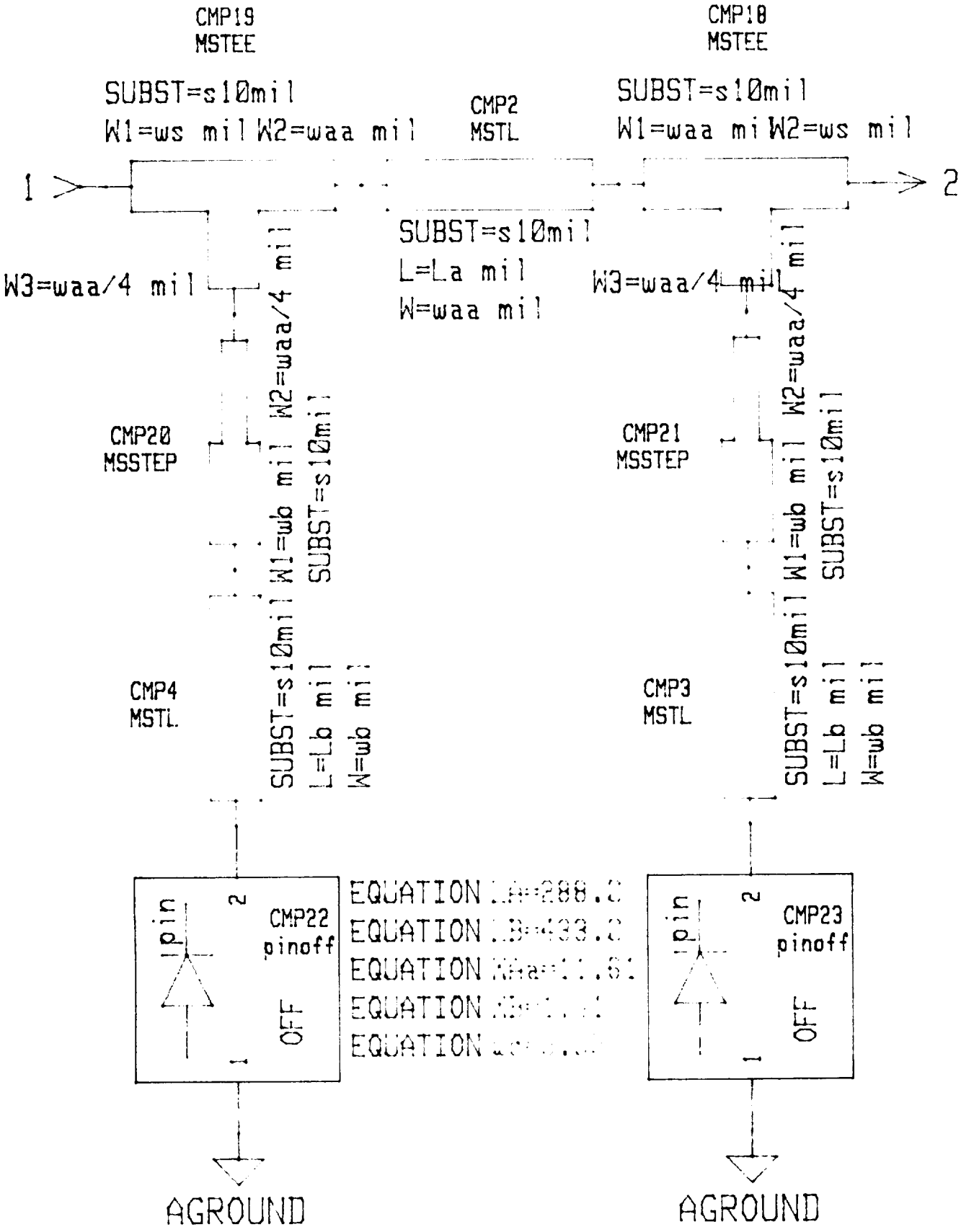

Fig. 7.b. Loaded-line 45°Phase Shifter Bit

ORIGINAL PAGE I
OF POOR QUALIT

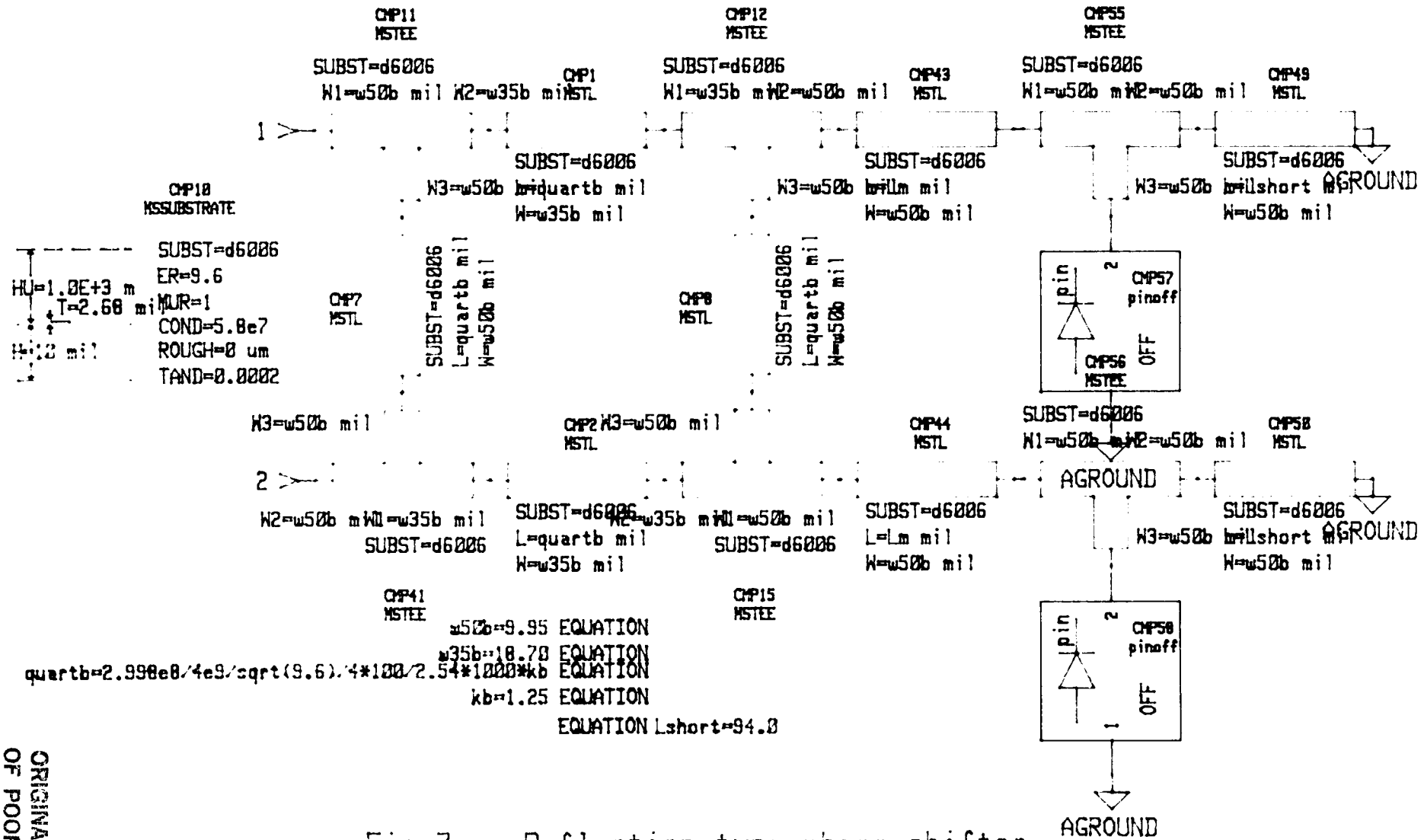

Fig.7.c. Reflection-type phase shifter

ORIGINAL PAGE IS
OF POOR QUALITY

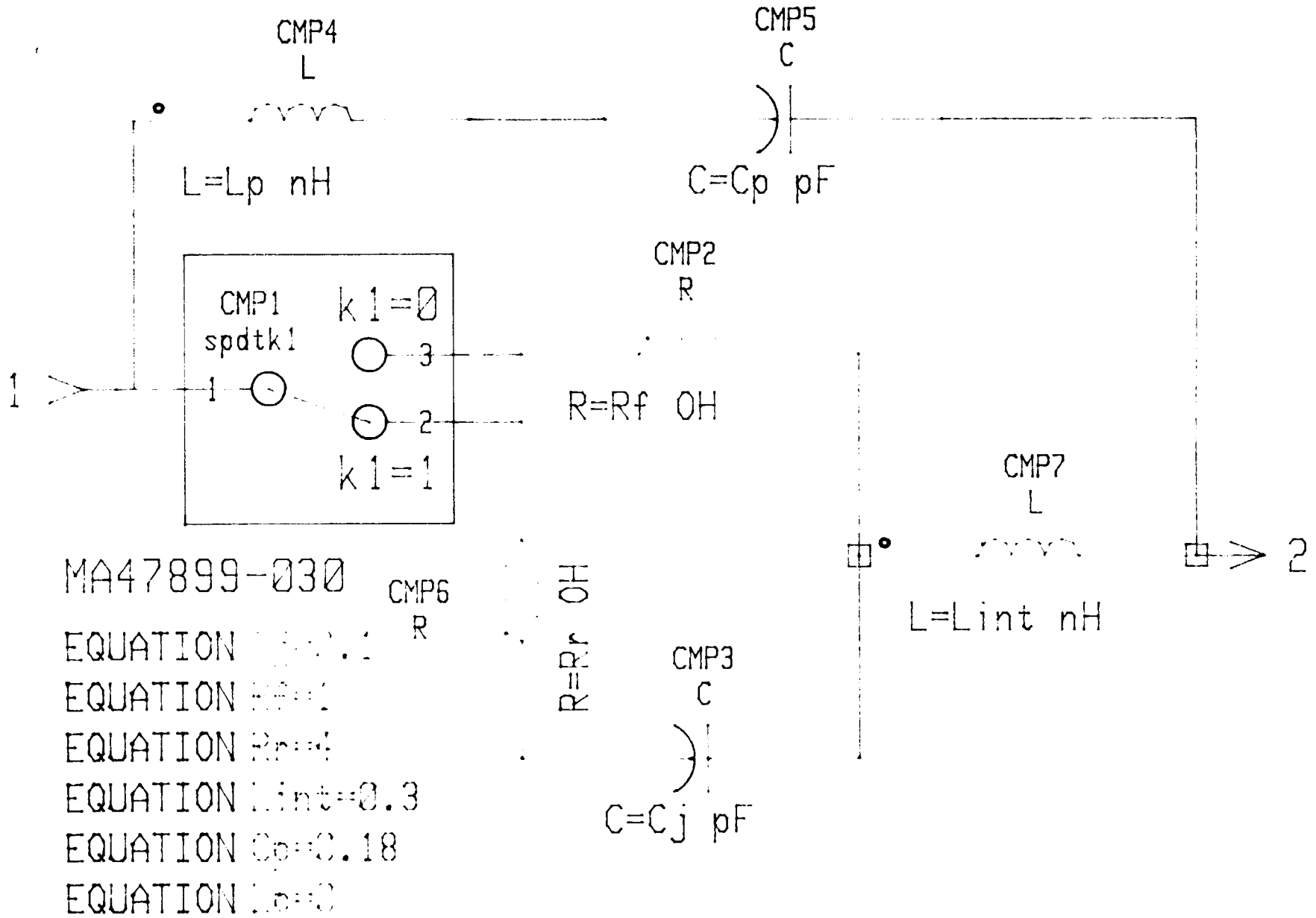

Fig. 8. Equivalent Circuit for a Packaged PIN-diode